Molecular Crystals and Liquid Crystals
Publication details, including instructions for authors and subscription information:
http://www.tandfonline.com/loi/gmcl16

Optical Behaviour of Mixtures of Nematic and Cholesteric Compounds

Nagappa D. Revannasiddaiah [a] & D. Krishnamurti [a]
[a] Department of Physics, University of Mysore, Mysore, 570 006, India
Version of record first published: 20 Apr 2011.

To cite this article: Nagappa D. Revannasiddaiah & D. Krishnamurti (1983): Optical Behaviour of Mixtures of Nematic and Cholesteric Compounds, Molecular Crystals and Liquid Crystals, 101:1-2, 103-127

To link to this article: http://dx.doi.org/10.1080/00268948308072485

Mol. Cryst. Liq. Cryst., 1983, Vol. 101, pp. 103–127
0026-8941/83/1012–0103/$18.50/0

Printed in the United States of America

Optical Behaviour of Mixtures of Nematic and Cholesteric Compounds

NAGAPPA, D. REVANNASIDDAIAH and D. KRISHNAMURTI

Department of Physics, University of Mysore, Mysore 570 006, India.

(*Received May 26, 1983*)

Studies have been carried out on the characteristic optical textures exhibited by mixtures of nematic and cholesteric compounds, namely, *N*-(*p*-propoxybenzylidene)*p*-pentylaniline (PBPA) and cholesteryl ethyl carbonate (CEC). Many of the textures are metastable and undergo a slow transformation at room temperature in the course of some days or weeks. The optical properties and textures observed near room temperature are characteristic of the cholesteric mesophase in the case of mixtures with concentrations of PBPA below 35% as also at the higher concentrations in the range of 90% and above. In the range of concentrations of PBPA lying between 40 and 90%, the optical textures observed near room temperature are characteristic of the smectic mesophase. Refractive index data obtained in the different cases confirm the above identifications. Wherever the cholesteric texture has a sufficiently large pitch, it is possible to observe the striped pattern characteristic of the periodic variation of the refractive index associated with the helicoidal arrangement of the molecules in cholesteric layers. Numerous other features like the fan and focal-conic textures, drops and diffraction effects are also illustrated.

1. INTRODUCTION

It is well-known that the molecular ordering in the cholesteric mesophase may be regarded as equivalent to a twisted nematic structure. In this context, it is of interest to investigate the modifications in the molecular ordering which ensue when nematogenic and cholesteric compounds are mixed together. Amongst the earlier investigations on this topic, particular reference must be made to the work of Saupe[1] who used mixtures of (*p*-methoxybenzylidene)*p*-*n*-butylaniline and cholesteryl nonanoate. Studies of this nature are carried out with greater convenience if one chooses compounds which exhibit meso-

morphism near room temperature. In one of our earlier investigations,[2] we had obtained the data with regard to the birefringence of *N*-(*p*-propoxybenzylidene)*p*-pentylaniline (PBPA) which is nematic near room temperature. PBPA is smectic below 23°C. The compound, cholesteryl ethyl carbonate (CEC) exhibits the cholesteric mesophase near room temperature. The present paper reports the results of our studies on mixtures of the above two compounds. Numerous photographs are included here to illustrate the various optical textures and other effects which are characteristic of the different phases. Many of the textures are metastable and undergo a slow transformation at room temperature in the course of some days or weeks.

2. EXPERIMENTAL

The chemicals used in this investigation are from M/s Eastman Organic Chemicals and Atomergic Chemetals, USA, with a given purity of 98% minimum (by non-aqueous titration). The transition temperatures T_{N-I} for PBPA (69.1°C) and T_{C-I} of CEC (103°C) were determined using the polarizing microscope and a specially constructed hot-stage. The transition points for our samples are slightly less than the values reported in the literature, being less by 2°C for PBPA[3] and 0.5°C for CEC.[4] The differences are attributable to traces of impurities usually present in commercial samples. For example, the nematic–isotropic transition temperatures reported in the literature[5-8] for MBBA vary by as much as 5°C, due to the samples being of different purities. Owing to the limited quantities of the substances available, mixtures of different concentrations were prepared using the commercial samples straightaway. Mixtures of about ten different concentrations were prepared. In the following, the concentrations are defined as the weight percentage of PBPA in the total weight of the mixture of PBPA and CEC. The clearing temperatures as a function of concentration are shown in Figure 1. The values are accurate to about ±0.5°C. The variation exhibits a minimum, as is usual in the case of mixtures.[9-11]

For the different mixtures prepared by us, the densities and the refractive indices were determined using the techniques described in our earlier papers.[12-14] Refractive indices in some cases were also determined using Abbe refractometer, because it was more convenient and helped us to confirm the values determined by the spectrometer method. The density data at different selected temperatures for some of the mixtures are shown in Figure 2 and the values are accurate to

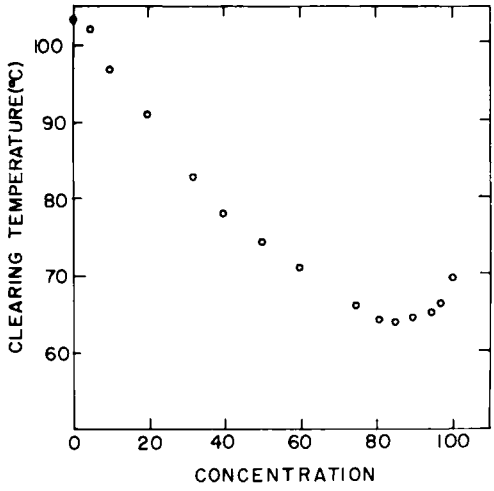

FIGURE 1 Clearing temperatures as a function of the weight percentage of PBPA in the mixture.

within ± 0.002 gm/cc. The sample of PBPA used here was the same as that with which we had carried out our earlier studies on birefringence and on Williams domains.[2,15] The index data for the sample of PBPA used in our calculations here are from our earlier studies.[2] The data for CEC had been reported earlier by Rettig *et al.*[16] and our data are in good agreement with theirs. The temperature variation of the refractive indices for $\lambda 5893$, for the sample of CEC used by us is

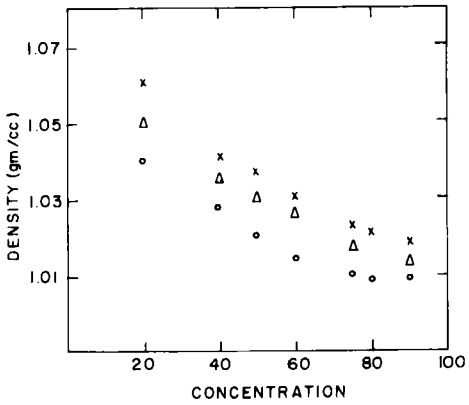

FIGURE 2 Variation of density with concentration at three different temperatures. (crosses: 30 °C, triangles: 41 °C, circles: 60 °C).

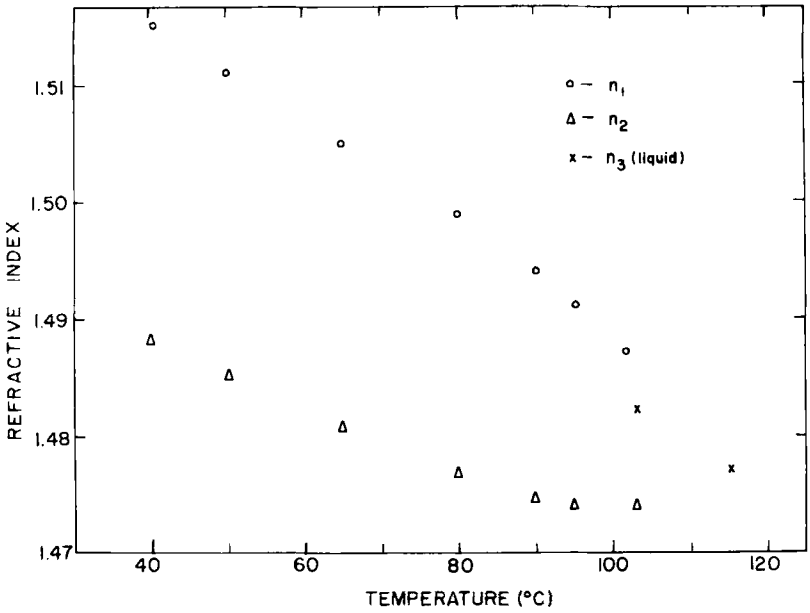

FIGURE 3 Temperature variation of the refractive indices of CEC. The values of the indices for the liquid phase and at temperatures above 70 °C are from Reference 16.

exhibited in Figure 3. The refractive indices of the mixtures at different temperatures are shown in Table I and the values are accurate to within ± 0.001.

3. VARIATION OF THE MEAN POLARIZABILITIES OF THE MIXTURES

The refractive indices in the liquid phase of the mixtures of different concentrations are also shown in Table I. Initially, in order to check up the consistency in the values of the densities and the refractive indices, the following calculations of the average polarizabilities of the mixtures were made. The respective mean polarizabilities of the molecules of PBPA and CEC α_a and α_b could be obtained using the Born relation (or the Lorenz–Lorentz relation in the case of the liquids). For the case of the mixtures, the refractive indices should satisfy the equation, viz.,

$$\frac{\overline{n^2} - 1}{\overline{n^2} + 2} = \frac{4\pi}{3}(N_a\alpha_a + N_b\alpha_b) = \frac{4\pi}{3}N\bar{\alpha}_{\text{mix}}, \qquad (1)$$

TABLE I

Refractive indices of the mixtures of PBPA and CEC for λ 5893 at different temperatures

Wt. % of PBPA		Temperature and refractive indices					
10	t(°C)	25	33	41	50	63	98
	n_1	1.537	1.532	1.529	1.524	1.520	1.490 (liquid)
	n_2	1.501	1.493	1.491	1.489	1.486	
20	t(°C)	26	34	42	52	58	92
	n_1	1.549	1.545	1.540	1.536	1.534	1.495 (liquid)
	n_2	1.499	1.499	1.497	1.495	1.494	
32	t(°C)	27	35	45	53	65	84
	n_1	1.555	1.553	1.548	1.544	1.536	1.498 (liquid)
	n_2	1.501	1.499	1.499	1.498	1.497	
40	t(°C)	35	43	50	55	61	78
	n_1	—	1.560	1.558	1.554	1.553	1.506 (liquid)
	n_2	1.499	1.505	1.504	1.504	1.503	
50	t(°C)	36	43	50	55	62	75.5
	n_1	—	1.570	1.559	1.557	1.554	1.519 (liquid)
	n_2	1.500	1.501	1.505	1.505	1.506	
60	t(°C)	30	40	50	55	61	72.5
	n_1	—	—	—	—	—	1.543 (liquid)
	n_2	1.504	1.505	1.507	1.508	1.513	
75	t(°C)	30	40	50	55	60	67.1
	n_1	—	—	—	—	—	1.549 (liquid)
	n_2	1.512	1.513	1.515	1.515	1.516	

where N_a and N_b are the number of molecules of PBPA and CEC respectively, in unit volume of the mixture. Here, $\overline{n^2}$ is the mean square of the principal refractive indices. For the cholesteric phase n_1 corresponds to the ordinary and n_2 to the extraordinary ray and $\overline{n^2} = (2n_1^2 + n_2^2)/3$. Further, $N\bar{\alpha}_{\text{mix}} = N_a\alpha_a + N_b\alpha_b$ and $N = N_a + N_b$. If one takes x_a gm of PBPA and x_b gm of CEC, then the number of molecules of PBPA per unit volume of the mixture which has a density

ρ_{mix} may easily seen to be given by

$$N_a = \frac{x_a}{x_a + x_b}\left(\frac{N_A}{M_a}\right)\rho_{mix}, \tag{2}$$

where M_a is the molecular weight of PBPA and N_A is the Avogadro number. Similarly, N_b, the number of molecules of CEC per unit volume of the mixture is given by

$$N_b = \frac{x_b}{x_a + x_b}\left(\frac{N_A}{M_b}\right)\rho_{mix}, \tag{3}$$

where M_b is the molecular weight of CEC. Therefore,

$$N = \left(\frac{x_a}{M_a} + \frac{x_b}{M_b}\right)\left(\frac{N_A}{x_a + x_b}\right)\rho_{mix}. \tag{4}$$

From the density data and the values of α_a and α_b it is possible to calculate the values of $\bar{\alpha}_{mix}$ using the relation $\bar{\alpha}_{mix} = (N_a\alpha_a + N_b\alpha_b)/(N_a + N_b)$ and from refractive index data. A comparison of the two sets of values leads to very good agreement as may be seen from Figure 4. The variation of $\bar{\alpha}_{mix}$ with the concentration of PBPA confirms the law of additivity of polarizabilities. It was also tested whether the density of the mixture in liquid phase would satisfy the

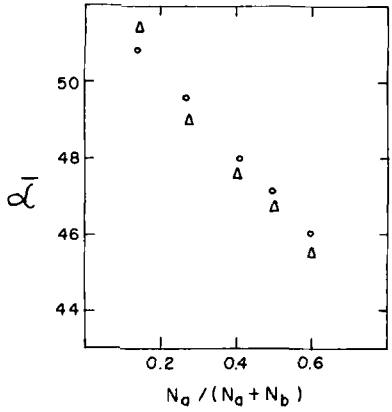

FIGURE 4 Mean polarizabilities $\bar{\alpha}_{mix}$ (in units of 10^{-24} cm^3) as a function of $N_a/(N_a + N_b)$ at a typical temperature of 62.3 °C for different mixtures. Circles: values calculated using Eqs. (1)–(4). Triangles: values from index data.

relation involving the additivity of volumes, i.e.,

$$\rho_{\text{mix}} = \frac{x_a + x_b}{(x_a/\rho_a) + (x_b/\rho_b)}. \tag{5}$$

Here, ρ_a and ρ_b refer to the densities of PBPA and CEC respectively. However, the law of additivity for volumes is not satisfied evidently because the different molecules of the mixture adjust suitably their relative orientation and packing, depending on the intermolecular interactions.

4. BIREFRINGENCE AND EFFECTIVE OPTICAL ANISOTROPY OF THE MIXTURES

It was possible to obtain the principal refractive indices n_1 and n_2 for all concentrations up to 50% of PBPA using Abbe refractometer. The refractive index n_1 corresponding to the ordinary ray is greater than the refractive index n_2 corresponding to the extraordinary ray, indicating that the material is uniaxial negative, as is characteristic of the cholesteric mesophase. A detailed discussion of the determination of the indices using the Abbe refractometer and the method of identification of n_1 and n_2 was given in an earlier paper on cholesteryl oleyl carbonate[17] (COC). The effective polarizabilities are calculated from the Lorenz-Lorentz formula. For example, for the extraordinary index n_2,

$$\frac{n_2^2 - 1}{n_2^2 + 2} = \frac{4\pi}{3} N\alpha_2(\text{mix}). \tag{6}$$

By using a correspondingly similar equation for n_1, it is possible to calculate the effective polarizability α_1 for the ordinary ray. For concentrations of PBPA up to 50%, the birefringence is relatively low. Hence, any anisotropy in the Lorentz field factors may be neglected and the use of the Lorenz-Lorentz relation is justifiable. The following conclusions emerge from our calculations. For a given concentration of the mixture in the range up to 50% of PBPA, the values of $(\alpha_1 - \alpha_2)$ exhibit a tendency for only a slight decrease with increase of temperature, indicating that there is no major change in the molecular ordering in the cholesteric phase with temperature. Further, with increasing concentration of PBPA, the values of $(\alpha_1 - \alpha_2)$ also increase because the effective optical anisotropy associated with the

molecules of PBPA is far greater than that associated with CEC. In fact, with mixtures having concentration of PBPA 60% and above, it is possible to determine only one refractive index which is identifiable with the ordinary ray. The numerical value here corresponds to the value of n_2 in the cholesteric phase, (see for example, at a concentration of about 50% PBPA and below). This indicates that the material here is optically uniaxial positive. This is possible only if the mesophase corresponds to the nematic or smectic. It emerges from the optical textures to be discussed in the following section, that the mesophase in such cases corresponds to the smectic phase. Sometimes at higher concentrations (for example at and above 90% PBPA) there appears a phase transition from the smectic to the cholesteric mesophase at the higher temperature as evidenced by a steep increase in the refractive index beyond 57 °C as may be seen in Figure 5 showing the data for a sample with 90% of PBPA. The drop in the refractive index beyond 60 °C may be explained as the prelude to the melting transition taking place at 64.5 °C.

Wherever both indices are available, the values of $(\alpha_1 - \alpha_2)$ may be calculated using the Lorenz-Lorentz relation. The calculated values

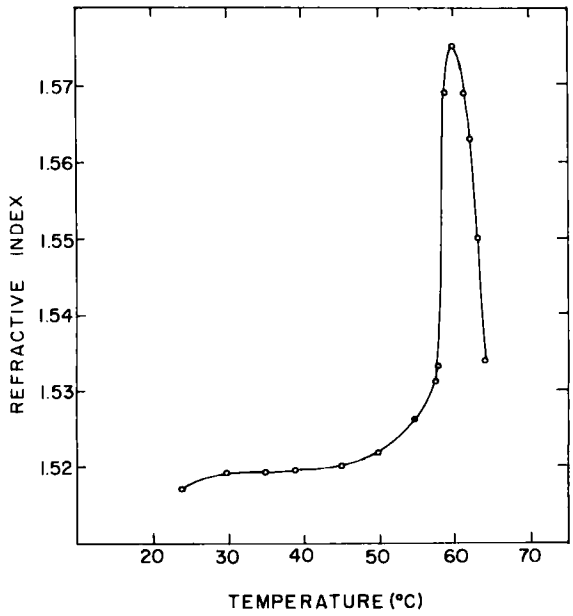

FIGURE 5 Temperature variation of the refractive index n_1 in the case of a mixture with 90% PBPA.

may be compared with that to be expected from additivity of the anisotropy of polarizabilities as expressed by the following relation

$$(\Delta\alpha)_{\text{mix}} = (\alpha_1 - \alpha_2)_{\text{mix}} = (N_a \Delta\alpha_a + N_b \Delta\alpha_b)/(N_a + N_b), \quad (7)$$

where $\Delta\alpha_a$ is equal to $(\alpha_e - \alpha_0)/2$ of PBPA at the corresponding temperature of the nematic phase and $\Delta\alpha_b$ is equal to $(\alpha_1 - \alpha_2)$ of CEC. The factor of half involved in the expression for $\Delta\alpha_a$ arises because the molecules of PBPA are arranged in the layers of the helicoidal structure of the cholesteric mesophase. From Eq. (7) it follows that

$$(\Delta\alpha)_{\text{mix}} - N_b \Delta\alpha_b/(N_a + N_b) = N_a \Delta\alpha_a/(N_a + N_b). \quad (8)$$

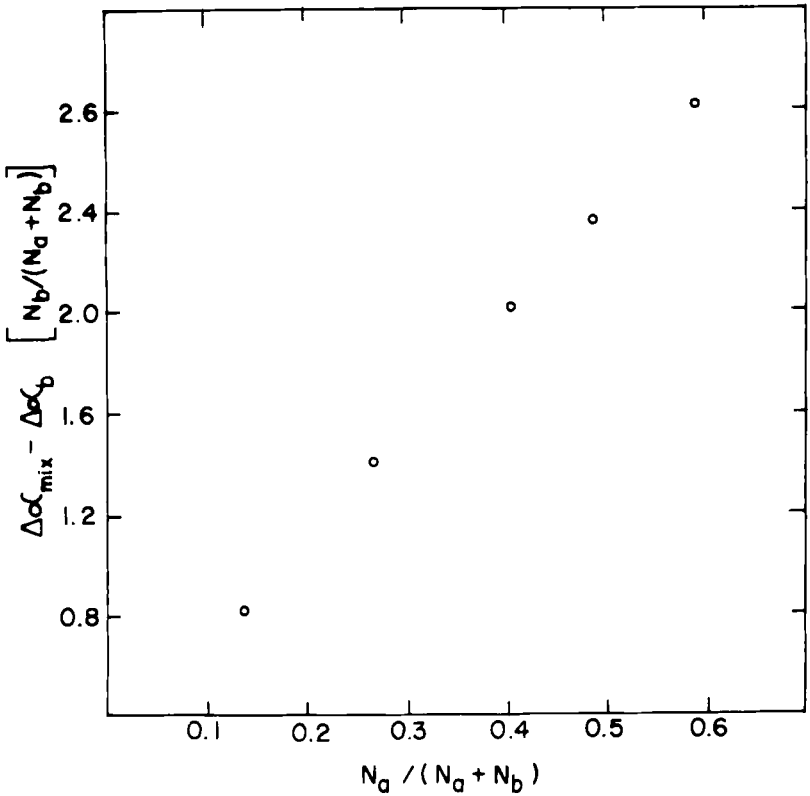

FIGURE 6 Variation of the optical anisotropy of mixtures with concentration. All the calculations are made using Eq. (8) at a typical temperature of 62.3°C. Here, values of $\Delta\alpha$ are in units of 10^{-24} cm^3.

Hence, a graph of the left hand side of the above equation versus $N_a/(N_a + N_b)$ should be linear, and this is actually the case in Figure 6. The slope of the graph is equal to 4.7×10^{-24} cm^3, this being almost half the value of $|(\alpha_e - \alpha_0)| = 9.96 \times 10^{-24}$ cm^3 for PBPA at 62.3°C, (see, Ref. 2).

5. OPTICAL TEXTURES

In the case of a pure cholesteryl compound (kept between slide and a cover glass), the planar texture is obtained in the cholesteric mesophase by a slight displacement of the cover glass. The planar texture is characterized by the specular reflection arising from the helicoidal structure which has a spatial periodicity which is of the order of the wavelength of light. In the case of CEC the specular reflection at room temperature corresponds to a wavelength lying in the deep-violet region. In the following, we are concerned with the optical textures exhibited by the mixtures and all the textures reproduced in this paper have been photographed at room temperature ($\simeq 30$°C). Many of the textures are metastable and undergo a slow transformation at room temperature in the course of some days or weeks.

Here, it is pertinent to mention that the cholesteric mesophase also exhibits the focal-conic texture. The focal-conic texture is also a characteristic of the smectic mesophase and the identification of the two phases can be made unambiguously from the fact that whereas the cholesteric mesophase is optically uniaxial negative, the smectic mesophase is uniaxial positive. Further, X-ray diffraction photographs obtained with the smectic mesophase exhibit a low angle diffraction ring associated with the spacing of the smectic layers, the spacing being of the order of the molecular length.

When a cholesteric compound is added as impurity to a nematic compound the pitch of the cholesteric mesophase decreases with increasing concentration of the cholesteric compound. Indeed, if the pitch is sufficiently large it is possible to observe under the polarizing microscope the stripes associated with the helicoidal structure superposed on the fan textures, clearly indicating that the mesophase is cholesteric (see for example Figure 7).

Very often the properties and optical textures observed near room temperature are characteristic of the cholesteric mesophase in the case of mixtures with concentrations of PBPA below 35%. Here, the medium is uniaxial negative.

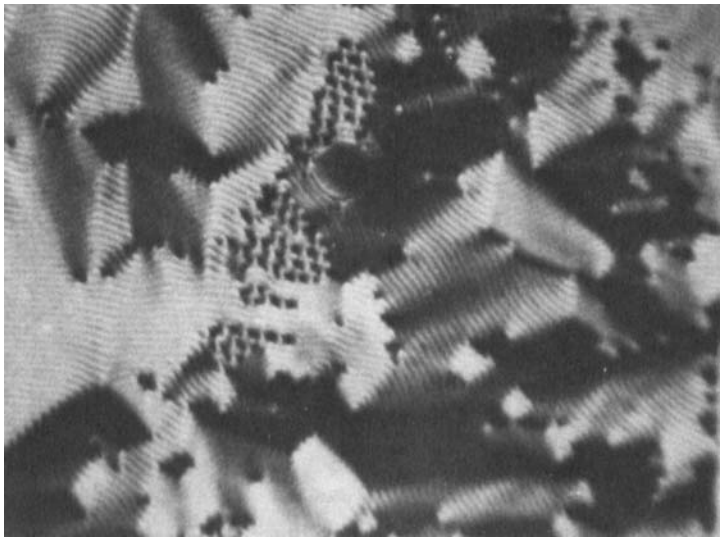

FIGURE 7 Microphotograph of a fan-shaped texture with stripes, exhibited by a specimen with 99% of PBPA. Crossed polars. 265 x

For observations of the optical texture, the sample was sandwiched between the slide and a cover glass and melted by keeping it in a hot-stage, the temperature of which can be controlled. The textures were observed under a polarizing microscope. The thickness of the samples were usually of the order of 25–50 microns. In the range of these thicknesses the textures were not dependent on the thickness of the sample. With larger thicknesses there was a tendency for the textures in different layers to overlap and give rise to a confusing pattern.

(a) Concentration of PBPA in the range of 0 and 40%

When the molten sample is cooled, the setting point is marked by the genesis of nucleation at several points which appear as minute bubbles initially, but which progressively grow radially as birefringent fibrillar textures, whose principal directions of refractive indices lie parallel and perpendicular to the radial fibrils. This texture (Figure 8) is somewhat similar to the radial fibrillar patterns which were observed by us in the case of spherulites.[18] However, here the radial fibrils are rather irregular. This form of the texture is stable only for a few

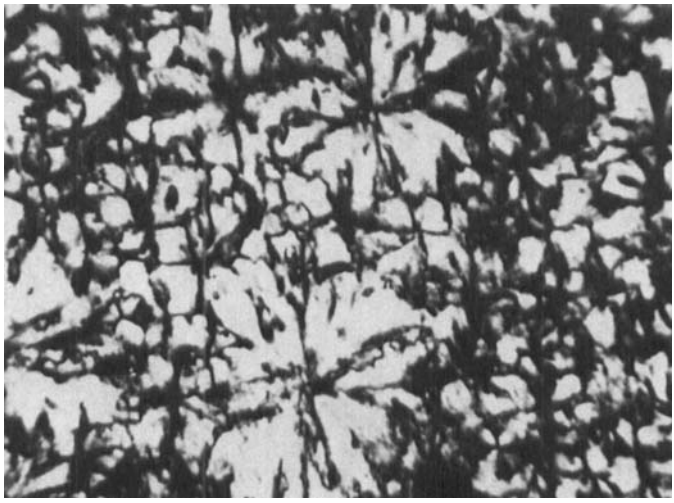

FIGURE 8 Microphotograph of a broken spherulite texture exhibited by a mixture with 5% of PBPA. Crossed polars. 570 x

minutes, but it was possible for us to obtain the V_V and H_V scattering patterns using the same experimental arrangement described in one of our earlier papers.[19] The V_V and the four leaf clover-shaped H_V patterns (see Figure 9) confirm the fact that the principal directions of the refractive indices were parallel and transverse to the radial fibrils.

The above mentioned radial fibrillar pattern undergoes a slow transformation at room temperature in the course of about twenty

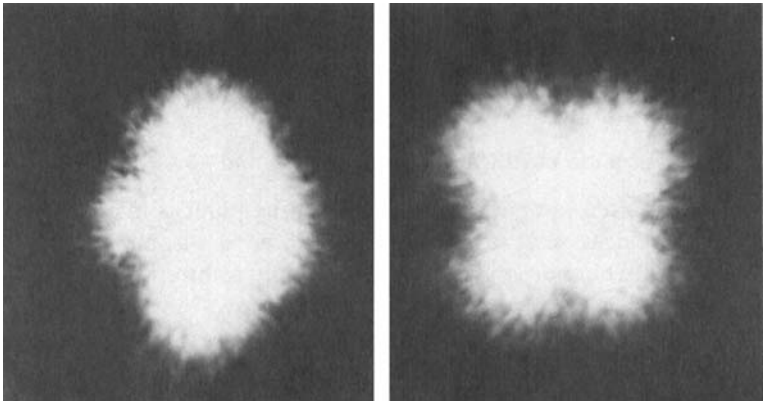

(a) (b)

FIGURE 9 Low angle optical scattering patterns exhibited by the texture in Figure 8. (a) V_V and (b) H_V.

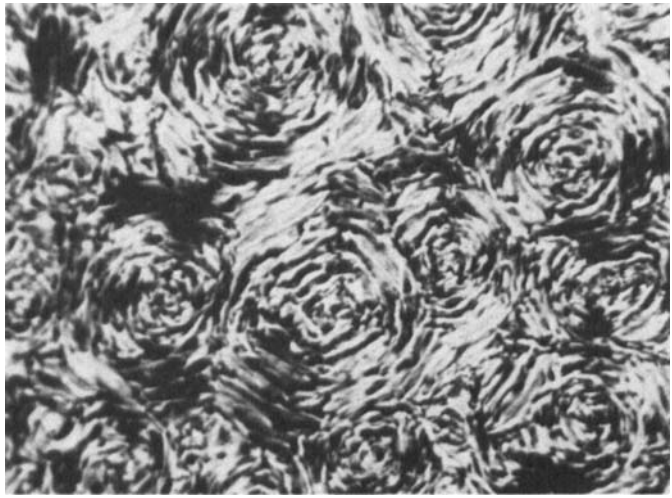

FIGURE 10 Microphotograph of the focal-conic texture exhibited by the specimen with 20% of PBPA. Crossed polars. 190 x.

minutes to give a focal-conic pattern consisting of domains arranged to form an irregular ringed structure (see Figure 10). In this case also we obtain low angle optical scattering patterns as in Figure 9, corresponding to the principal directions of the indices lying radially and tangentially to the irregular ringed pattern. The above patterns were observed for the specimen between the slide and the cover glass.

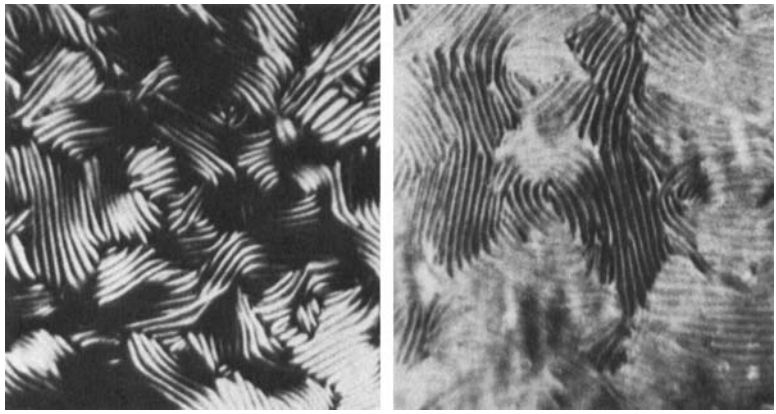

FIGURE 11 Microphotograph of a uniformly spaced striped pattern exhibited by a mixture with 20% of PBPA, (Specimen with a free-surface). (a) Specimen between crossed polars. 425 x. (b) Using incident polarized light with the electric vector along the vertical. The striped pattern is indistinct along the horizontal direction. 425 x

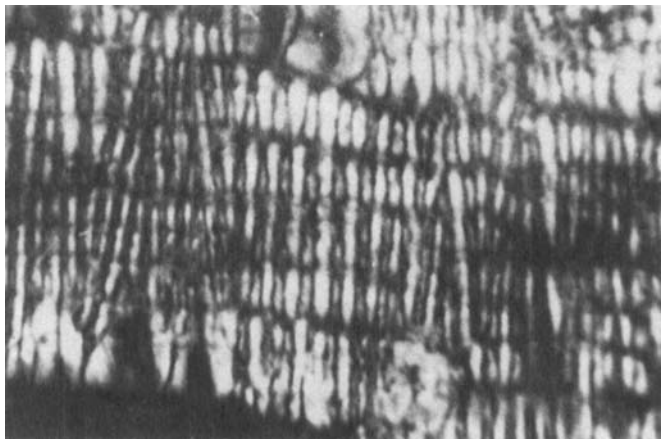

FIGURE 12 Microphotograph of the focal-conic texture exhibited by a specimen with 32% of PBPA. Crossed polars. 1270 x

On the other hand, outside the cover glass a pattern consisting of highly uniformly spaced stripes is observed, (see for example Figure 11a). When only the polarizer was used, the stripes were observed with maximum contrast in regions where the length of the stripes were parallel to the vibration direction of the polarizer as may be seen from Figure 11b. The above feature has its origin in the periodic variation

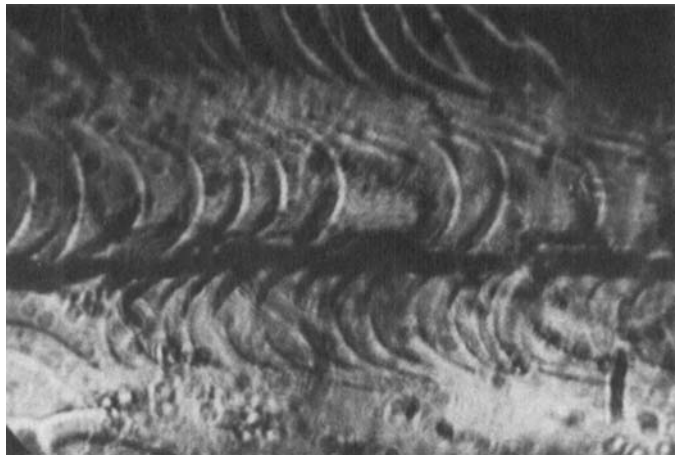

FIGURE 13 Microphotograph showing steps exhibited by the free surface of a specimen with 32% of PBPA. Crossed polars. 570 x

of the refractive index of the medium along the direction perpendicular to the stripes, for light polarized with its vibration direction tangential to the stripes. Such a periodic variation of the refractive index arises because the molecular order has a helicoidal structure, the axis of the helix being in the plane of the slide and perpendicular to the stripes. There is a close analogy between the facts reported here and those reported earlier by us in the case of spherulites.[18,19]

The texture showing the irregular ringed structure in Figure 10 is also metastable and undergoes a transformation to what appears to be the smectic mesophase which is also characterized by focal-conics. The textures are shown in Figure 12, and these are similar to the case of the focal-conics in smectic mesophase of dodecyl benzene sulphonic acid and its sodium salt,[20] (see, Figure 9b in that paper). Outside the cover glass the striped pattern of Figure 11 undergoes a slow transformation to stepped drops, (see for example, Figure 13). The X-ray diffraction pattern of the texture at this stage exhibits a small angle ring and a diffuse large angle ring, as shown in Figure 14, confirming that the texture corresponds to the smectic A phase.

(b) Concentrations of PBPA in the range of 40 and 90%

In the case of mixtures with concentration of PBPA in the range 40% and above, the mesophase at room temperature is characterized by the

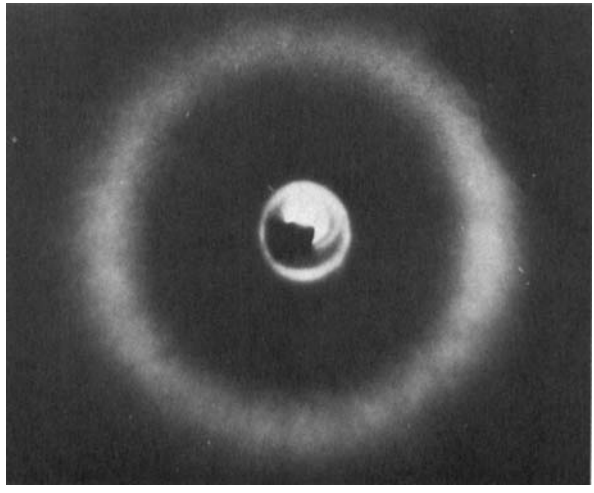

FIGURE 14 X-ray diffraction pattern of a mixture with 40% PBPA, using Cu–K_α radiation.

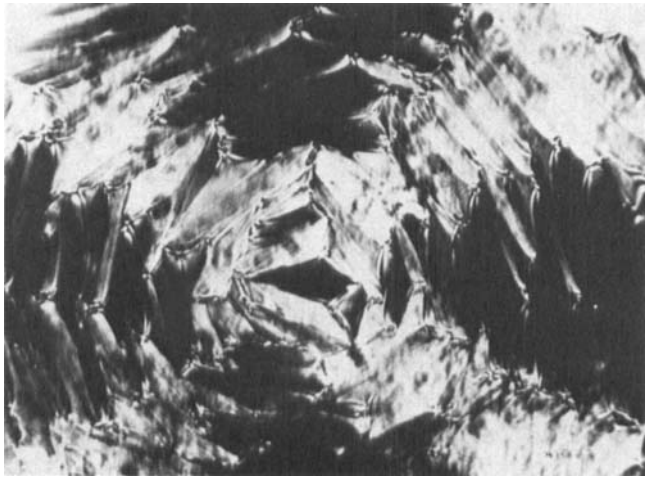

FIGURE 15 Microphotograph of the focal-conic texture exhibited by a specimen with 50% of PBPA. Crossed polars. 520 x. This figure is similar to Figure 10.

focal-conic texture shown in Figure 15, which figure is similar to Figure 10, but with the difference that the focal-conic domains are larger. In all the cases discussed here, the texture is metastable to varying degrees in so far as the time it takes for the gradual transformation to the next texture is different for different concentrations, and the time is of the order of a few days. The texture in Figure 15 is slowly transformed to the texture exhibiting the ellipses shown in

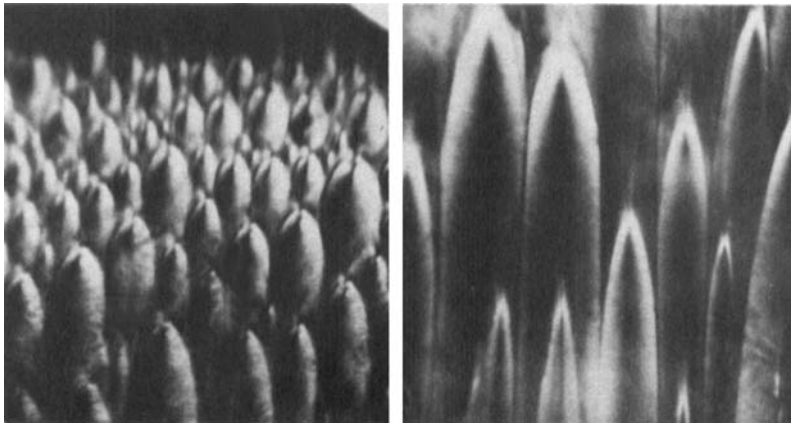

(a) (b)

FIGURE 16 Microphotographs of the focal-conic domains exhibited by mixtures with (a) 50% of PBPA and (b) 85% of PBPA. Crossed polars. 500 x

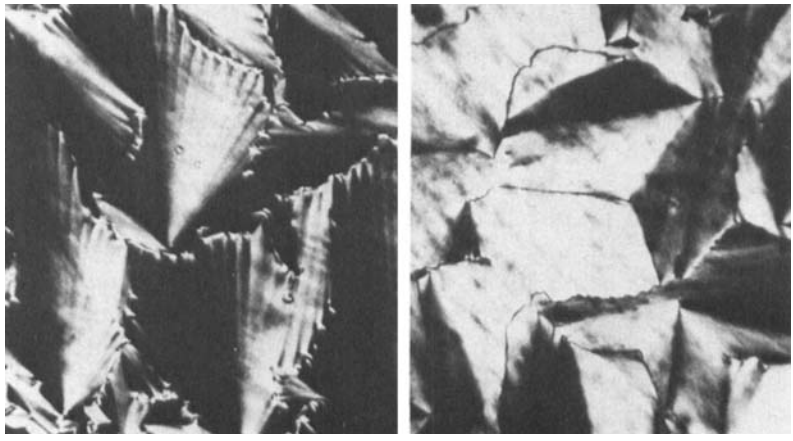

(a) (b)

FIGURE 17 Microphotograph of the fan shaped patterns exhibited by mixtures as observed between crossed polars. (a) with 80% of PBPA. 220 x. (b) with 60% of PBPA. 520 x

Figures 16(a) and 16(b). Even this texture is transformed to the characteristic fan-shaped texture, see, Figures 17(a) and 17(b) associated with the smectic mesophase in the course of about ten days. The X-ray diffraction pattern of this phase is characteristic of the smectic A phase as in Figure 14. Ultimately, crystallization occurs with the formation of the mosaic textures shown in Figure 18.

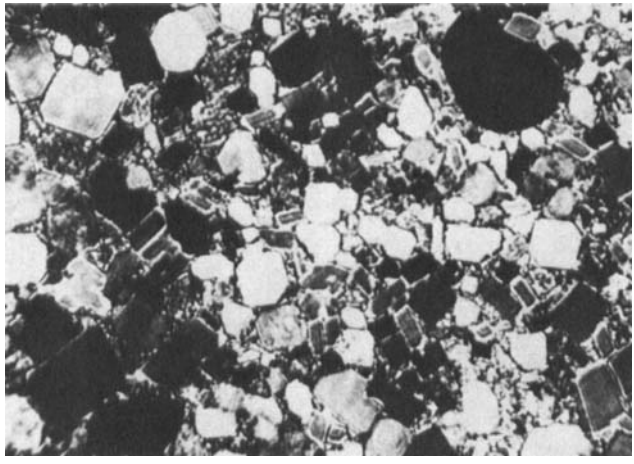

FIGURE 18 Microphotograph of a mosaic texture obtained with a specimen with 60% of PBPA. Crossed polars. 175 x

(c) Concentration of PBPA in the range of 90 and above

Unlike the cases discussed hitherto, in the range of concentration of PBPA lying between 90% and above the optical textures correspond to only the cholesteric mesophase with large values for the pitch. The striped patterns are the textures frequently observed. It is confirmed that there is a periodic variation of the refractive index for the light polarized along the direction of the stripes. In fact, the visibility of the stripes is poor when the incident light is polarized along the direction transverse to the length of the stripes. The characteristic striped pattern also gives rise to optical diffraction when light is propagating along the direction parallel to the cholesteric layers. The features are illustrated in Figures 19(a) and 19(b). The periodic variation of the refractive index is also confirmed from interference experiments similar to that carried out by us in the case of spherulites.[19] Figure 20(a) represents a finger print pattern. Figure 20(b) shows the spectrum of white light transmitted through the optical arrangement consisting of a quartz crystal and the specimen with the finger print pattern placed between crossed polars with the stripes perpendicular to the slit of the spectrograph. The sinusoidal dark bands in Figure 20(b) indicate the sinusoidal variation in the retardation arising as a consequence of the periodic variation of the refractive index. The details of the experimental set up are the same as given in an earlier paper.[19]

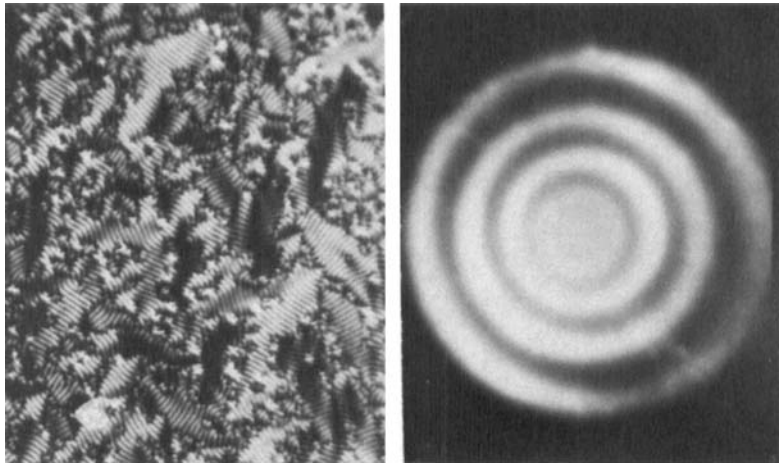

FIGURE 19 (a) Microphotograph of a striped pattern exhibited by a specimen with 99% of PBPA. Crossed polars. 190 x. (b) Optical diffraction pattern exhibited by the striped texture shown in Figure 19(a). Photograph was obtained using light of wavelength 5461 A.

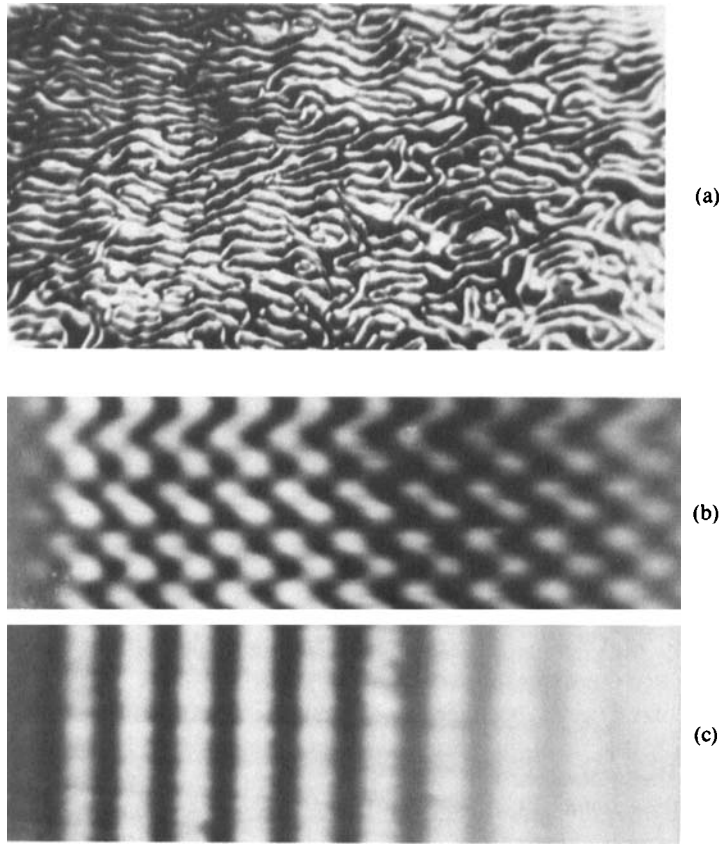

FIGURE 20 (a) Finger print pattern obtained with a specimen containing 99% of PBPA. 570 x. (b) Banded spectrum consisting of sinusoidal bands obtained with the same texture [Figure 20(a)] and with quartz crystal kept between crossed polars. (c) Reference banded spectrum obtained when only the quartz crystal (thickness = 0.25 cm) is kept between crossed polars. The left hand side is the red region of the spectrum.

(d) Some characteristic features of 'drops'

It is well-known that the cholesteric and smectic mesophases exhibit stepped drops with free surface. One encounters less frequently spherical 'drops' with a radial molecular arrangement in the case of specimens between slide and cover glass. A typical free stepped drop in the cholesteric mesophase is exhibited in Figures 21(a) and 21(b). Figure 21(a) was obtained using plane polarized light, whereas Figure 21(b) was photographed with the sample between crossed polars. Figure 21(a) shows the steps. When observed between crossed polars the drop

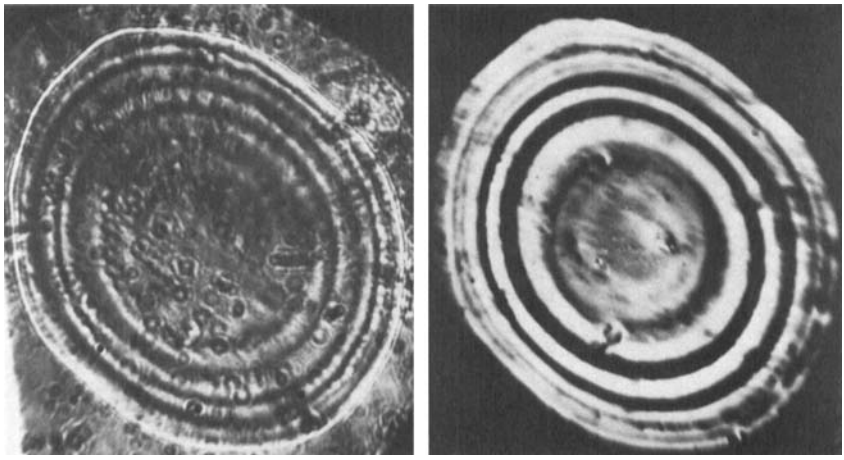

(a) (b)

FIGURE 21 Microphotographs of a free cholesteric drop obtained with a specimen having 99% of PBPA. (a) Using plane polarized white light. 150 x. (b) Using sodium yellow light and with the specimen between crossed polars. 140 x

exhibits dark rings as shown in Figure 21(b). Each dark ring corresponds to a contour of equal thickness and the successive extinctions correspond to a change in optical rotation by an angle of π. The optical rotation can be observed by keeping the drop between crossed or parallel polars and by observing the spectrum of the transmitted white light, when the image of the drop is focused on the slit of the spectrograph. The periphery of the drop which is thinner than the central portion, shows the extinction at lower wavelengths. The rotation is larger for the lower wavelengths and hence the extinction which corresponds to a given rotation occurs at lower wavelengths for the thinner regions of the drop. On the other hand, the extinction shifts to relatively longer wavelengths at the centre of the drop, because here the thickness of the drop is large and the same rotation is achieved at the longer wavelengths. These features are illustrated in Figures 22(a) and 22(b).

Spherical 'droplets' are observed occasionally between slide and cover glass in the case of mixtures having concentration of PBPA lying between 60 percent and above. The crossed extinctions obtained with these indicate the radial spherulite-like molecular arrangement in either smectic or cholesteric layers. Figures 23(a), 23(b) and 23(c) illustrate the above features. However, it may be pointed out that no striped pattern is seen with these drops. Occasionally, it is possible to

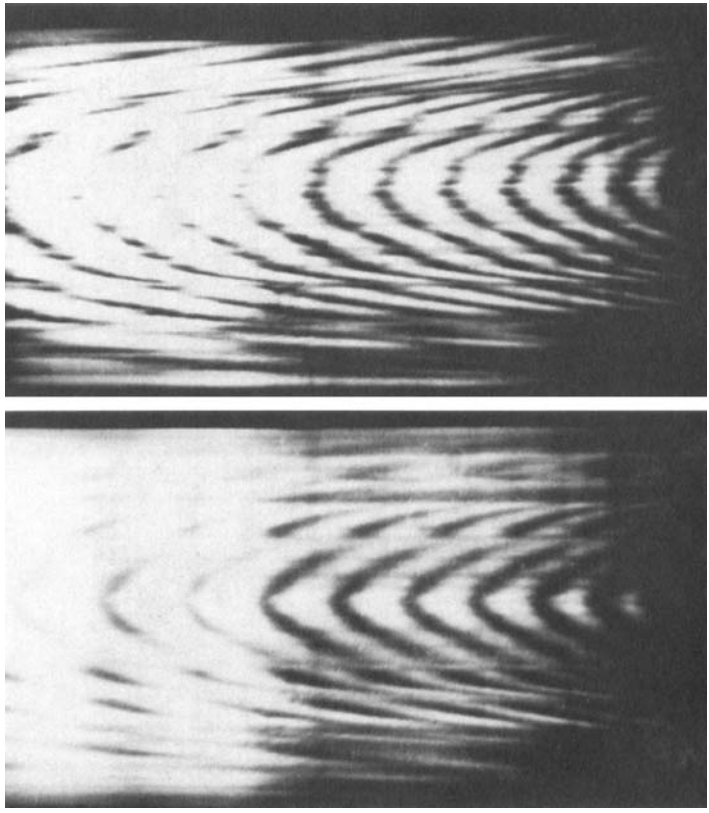

FIGURE 22 Dark bands of extinction in the spectrum of white light transmitted through the 'cholesteric drop' shown in Figure 21. The photographs were obtained (a) With the specimen between crossed polars. The left hand side of the spectrum corresponds to the red region. In the dark bands the discontinuities occur at the steps. (b) With the vibration directions of both the polarizer and the analyzer vertical.

observe droplets with striped pattern (as in Figure 24) presenting an end-on view of the cholesteric layers with periodic variation of the refractive index for electric vector along the directions of the stripes. These drops are analogous to the drops observed with PBLG.[21]

The pitch of the cholesteric arrangement was measured wherever possible using the optical diffraction pattern or the striped pattern and Figure 25 exhibits the variation of the pitch with the concentration of PBPA. This is in conformity with the rule that for small concentration of cholesteryl compounds in nematics the pitch should be inversely proportional to the concentration of the cholesteryl compound.[22]

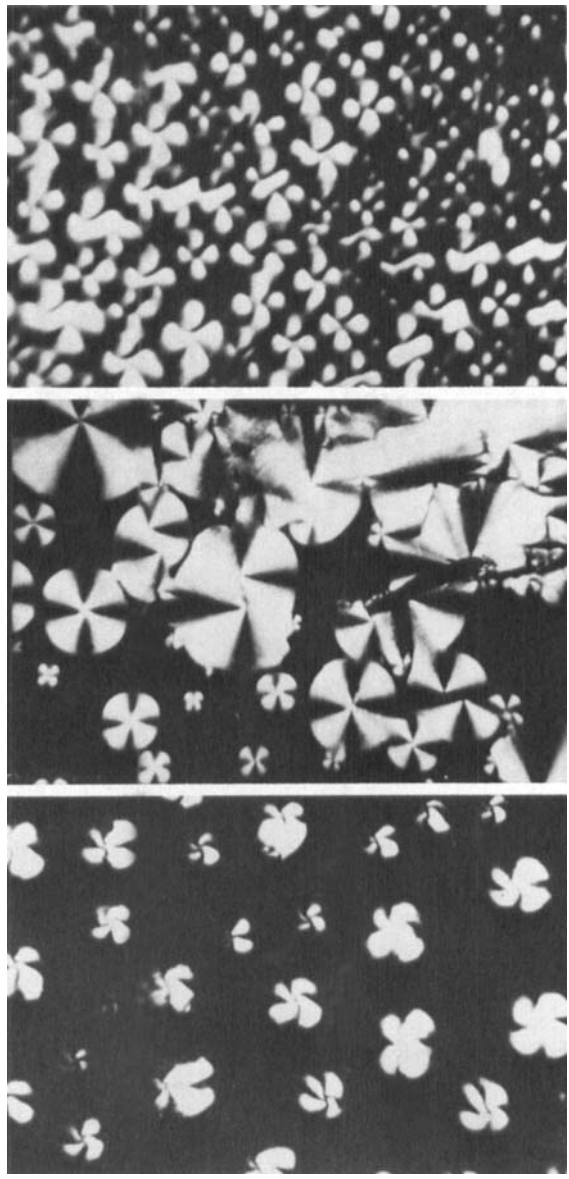

FIGURE 23 Microphotographs of 'spherical droplets' exhibited by different mixtures between crossed polars. (a) with 75% of PBPA. 695 x; (b) with 85% of PBPA. 400 x; (c) with 99% of PBPA. 610 x

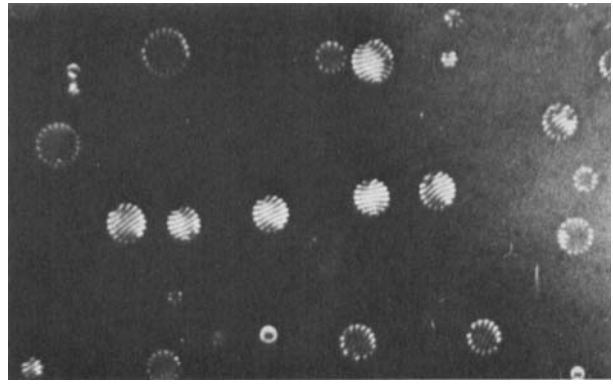

FIGURE 24 Microphotograph of 'droplets' with stripes exhibited by the mixture containing 99% of PBPA. Crossed polars. 265 x

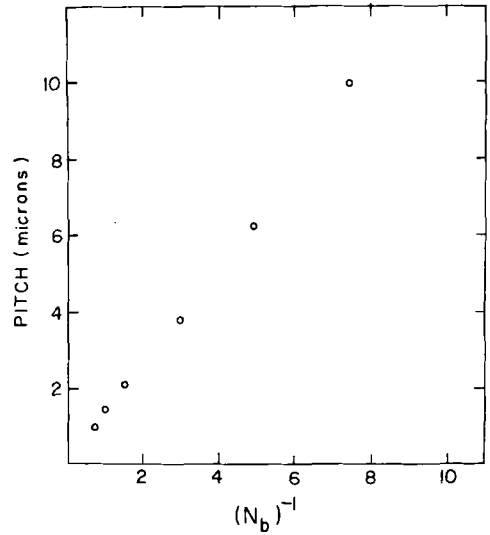

FIGURE 25 Variation of the pitch of the cholesteric mixture with the concentration of CEC in the range of 0 to 10%. Here, N_b represents the number of molecules of CEC per unit volume of the mixture. The values of N_b are in units of 10^{19}/cc.

6. CONCLUDING REMARKS

The above studies, apart from revealing numerous beautiful textures associated with the various cases, have enabled us to reach the following conclusions. (i) For mixtures with concentrations of PBPA 90% and above, the optical textures near room temperature are characteristic of the cholesteric phase. The periodic variation of the refractive index gives rise to diffraction effects and the striped texture. Stepped drops are observed here. (ii) In the region of the intermediate concentrations between 40 and 90% of PBPA the mesophase at room temperature often corresponds to the Smectic A mesophase as evidenced by the characteristic textures, X-ray diffraction pattern and the optical properties. (iii) In the region of concentration between 0 and 40% of PBPA the mesophase corresponds to the cholesteric phase as evidenced by the uniaxial negative character of the medium. However, it is not possible to exactly specify the concentrations up to which the mesophase is cholesteric because the mesophase which is cholesteric at the higher temperatures slowly transform to the smectic mesophase at room temperature. The slow transformations of the textures indicate the metastable nature of the intermediate textures. All the textures characteristic of the mesophase are transformed finally at room temperature to the mosaic textures characteristic of the crystalline phase.

Acknowledgments

One of us (Nagappa) acknowledges with thanks the award of a fellowship under the 'Faculty Improvement Programme' of the University Grants Commission, India.

References

1. A. Saupe, *Mol. Cryst. Liq. Cryst.*, **21**, 211 (1973).
2. D. Revannasiddaiah and D. Krishnamurti, *Mol. Cryst. Liq. Cryst.*, **53**, 63 (1979).
3. G. W. Smith, Z. G. Gardlund and R. J. Curtis, *Mol. Cryst. Liq. Cryst.*, **19**, 327 (1973).
4. D. Demus and G. Wartenberg, Pramāna Suppl. No. 1, p. 363 (1975).
5. I. Haller, H. A. Huggins and M. J. Freiser, *Mol. Cryst. Liq. Cryst.*, **16**, 53 (1972).
6. G. Vergoten and G. Fleury, *Mol. Cryst. Liq. Cryst.*, **30**, 213 (1975).
7. R. T. Thompson, D. W. Kydon and M. M. Pinter, *Mol. Cryst. Liq. Cryst.*, **39**, 123 (1977).
8. K. Hirakawa and S. Kai, *Mol. Cryst. Liq. Cryst.*, **40**, 261 (1977).
9. D. Krishnamurti, K. S. Krishnamurthy and R. Shashidhar, "Liquid Crystals-2", Part II p. 619, Ed. G. H. Brown, (Gordon and Breach Science Publishers, London, New York, Paris, 1969).
10. J. W. Goodby and G. W. Gray, *Mol. Cryst. Liq. Cryst.*, **48**, 127 (1978).

11. P. L. Finn and P. E. Cladis, *Mol. Cryst. Liq. Cryst.*, **84**, 159 (1982).
12. N. V. Madhusudana, R. Shashidhar and S. Chandrasekhar, *Mol. Cryst. Liq. Cryst.*, **13**, 61 (1971).
13. J. Shashidhara Prasad and H. S. Subramhanyam, *Mol. Cryst. Liq. Cryst.*, **33**, 77 (1976).
14. R. Somashekar, D. Revannasiddaiah, M. S. Madhava, H. S. Subramhanyam and D. Krishnamurti, *Mol. Cryst. Liq. Cryst.*, **45**, 243 (1978).
15. D. Krishnamurti and D. Revannasiddaiah, *Mol. Cryst. Liq. Cryst.*, **55**, 33 (1979).
16. R. Rettig, G. Pelzl and D. Demus, *J. Prakt. Chem.*, **318**, 450 (1976).
17. R. Somashekar and D. Krishnamurti, *Mol. Cryst. Liq. Cryst.*, **84**, 31 (1982).
18. D. Revannasiddaiah, M. S. Madhava and D. Krishnamurti, *Mol. Cryst. Liq. Cryst.*, **39**, 87 (1977).
19. D. Krishnamurti, M. S. Madhava and D. Revannasiddaiah, *Mol. Cryst. Liq. Cryst.*, **47**, 153 (1978).
20. D. Krishnamurti and R. Somashekar, *Mol. Cryst. Liq. Cryst.*, **65**, 3 (1981).
21. G. W. Gray and P. A. Winsor, "Liquid Crystals and Plastic Crystals", Vol. 1, p. 179 (1974). (John Wiley and Sons Inc. New York, London, Sydney, Toronto).
22. P. G. de Gennes, "The Physics of Liquid Crystals" (Clarendon Press, Oxford, 1974) p. 239.